International Journal of Thin Films Science and Technology

http://dx.doi.org/10.18576/ijtfst/070103

Structural, Optical, Luminescence and Morphological Properties of Rod Shaped CdO Biotemplate Synthesized by Via Hen egg-Albumen Extract for Anti-Cervical Cancer Application

K. Mohanraj[1], *D. Balasubramanian*[1*], *N. Jhansi*[1], *M. Saravanabhavan*[2] *and J. Chandrasekaran*[3]

[1]Raman Research Laboratory, PG & Research Department of Physics, Government Arts College, Tiruvannamalai-606603, Tamilnadu, India.
[2]Department of Chemistry, Dr. NGP Institute of Technology, Coimbatore 641048, Tamilnadu, India.
[3]Department of Physics, Sri Ramakrishna Mission Vidyalaya College of Arts and Science, Coimbatore 20, Tamilnadu, India.

Received: 15 Sep. 2017, Revised: 22 Dec. 2017, Accepted: 27 Dec. 2017.
Published online: 1 Jan. 2018.

Abstract: In this work, the CdO biotemplate nanorods were synthesized by chemical rout assisted microwave irradiation method via Hen egg-albumin extract. The CdO biotemplate nanorods were characterized by various characterization techniques such as X-ray diffraction analysis (XRD), Fourier transform infrared spectroscopy (FTIR), High resolution scanning electron microscope (HRSEM), Transmission electron microscope (TEM), Energy dispersive X-rays spectroscopy (EDX), Ultra violet-Vis diffused reflectance spectroscopy (UV-Vis-DRS) and Photoluminescence spectroscopy (PL). The XRD patterns of CdO biotemplate nanorods show in cubic phase structure with average particle size 21-23 nm. Functional groups present in the compound were analyzed by FTIR technique. The HRSEM photograph shows the rod shape morphology. TEM images of CdO biotemplate confirm the rod shape morphology. The CdO biotemplate nanorods optical properties were studied by UV-Vis-DRS and PL. The current-voltage (I-V) properties are studied by DC conductivity. The CdO biotemplate possessed potent cytotoxicity against HeLa cancer cell line.
Keywords: Biotemplate, Structural properties, Optical properties, Cytotoxicity effect

1 Introduction

Metal oxide semiconductor nanoparticles are focused by the researchers in order to develop semiconductor device applications. CdO nanoparticles possess unique electrical, optical, chemical and physical properties. They have direct band gap energy 2.5eV and indirect band gap energy 1.98eV. So researchers are interested in preparing the CdO nanoparticles [1,2]. The CdO nanoparticles have wide application in solar cells, gas sensors, transparent electrodes, photo diodes, catalysts and optoelectronic devices [3,11].

Synthesizing metal oxide nanoparticles by microwave irradiation method has a greater advantage compared with microwave emulsion [12], chemical precipitation [13], Sonochemical, hydrothermal techniques [14], solvothermal process [15], mechanical process [16,18], and also chemical synthesis method [19,22].CdO nanoparticles are synthesized by microwave irradiation method (MWIM) with the use of egg albumen as a biotemplate. This method is a cheapest and easier method to prepare CdO nanoparticles. Here, we used egg albumen as a biotemplate due to its gelling, foaming and emulsifying character. Also, it has long amino acid chain. It can dissolve in water and bind the metal ions to good shape [23-24]. The nanoparticles synthesized by comparing egg-white with metal ions such as Mn2+/Mn3+, Fe2+/Fe3+, Cu2+, Zn2+ have interesting properties, which are already reported[25,30].

In this paper, CdO biotemplates were prepared by chemical rout assisted microwave irradiation method. The synthesized materials are subjected to various characteristic techniques.

2 Experimental Procedure

2.1 Materials

Cadmium chloride (CdCl2) and ammonia (NH4OH) solution were purchased from (Merck, 98%) Mumbai, India. All the Chemicals were of analytical reagent grade (AR grade) and used as received without purification. Hen

*Corresponding author E-mail: balad67@rediffmail.com

egg purchased in local market treated with double distilled water was used for the experiment.

2.2 Synthesis

For the synthesis of CdO nanostructure by microwave irradiation method using a staring 0.1M, cadmium hydroxyl solution was prepared by dissolving Cadmium chloride in double distilled water. 5ml freshly extracted albumen was mixed with double distilled water and stirred. The obtained albumen solution was added drop wise to the cadmium hydroxyl solution. pH of the solution is maintained at 8 by adding ammonia hydroxyl drop wise. The obtained product was washed several times with double distilled water and ethanol. The precipitate was irradiated for 5 minutes in a household micro oven (radiation frequency 2.45GHZ, power up to 1KW) with convection mode, a white color powder is obtained which is annealed at 300oC for 5 hrs using a muffle furnace.

2.3 Materials Characterizations

The CdO microstructure was analyzed by XRD using a Bruker AXS D8 Advance instrument and the monochromatic CuKα1 wavelength of 1.5406Å. The average crystalline size of crystallite was calculated using Scherrer's formula, $d = \frac{K\lambda}{\beta\cos\theta}$, where d is the mean crystalline size, K is a grain shape dependent constant (0.9), λ is the wavelength of the incident beam, θ is a Bragg reflection angle, and β is the full width at half maximum (FWHM) of the main diffraction peak. The functional groups were identified by Fourier transform infrared spectrometer (FTIR) using a Perkin Elmer- spectrometer ATR technique. The morphology and presence of CdO were investigated by High resolution scanning electron microscopy (HRSEM), using a JEOL 5600LV microscope at an accelerating voltage of 10kV. High resolution transmission electron microscopy (HRTEM) images and selected area electron diffraction pattern were recorded by using a Tecnai G20-stwin of accelerating voltage of 200kV. Thermal analysis was done using a thermogravimetric and differential thermal analyzer (TG-DTA Netzsch- model STA 409PC). The ultraviolet-visible (UV) spectrum is recorded by using a Perkin Elmer UV-Visible spectrometer. The room temperature PL was recorded by using spectrofluorometer instrument (JY Fluorolog-FL3-11). The DC electrical conductivity was measured using the Keithley electrometer 6517B two probe setup.

3 Results and Discussion

3.1 X-ray Diffraction Studies

The as prepared and 300oC annealed CdO biotemplates XRD patterns are shown in fig 1(a, b). The XRD patterns of the sample (a) and sample (b) showed the presence of CdO nanoparticles with cubic phase structure (JCPDS #39-1221). The following miller indices (111), (200), (210), (211), (220), (311), (222), (400), (331) observed at corresponding different diffraction peaks value are given in table 1. The Debye Scherrer formula, $d = \frac{K\lambda}{\beta\cos\theta}$ is used to calculate the average crystalline size of CdO nanoparticles and found to be 23 nm and 21 nm for the sample (a) & sample (b) respectively. The lattice parameter was calculated using following equation (1),

$$\frac{1}{d_{hkl}} = \left[\left(\frac{h^2 + k^2 + l^2}{a^2}\right)\right]^{1/2} \quad (1)$$

Where d is the d-spacing value, h, k and l are Miller indices, a- is the lattice parameter. The calculated lattice parameter for the sample (a) and (b), a= 5.1613Å, a= 5.4205Å and the values matches well with standard JCPDS file no #39-1221. The XRD measurements indicate the good crystalline nature of CdO nanoparticles product obtained and 300oC annealed sample (b) has higher crystallinity than the as prepared sample (a).

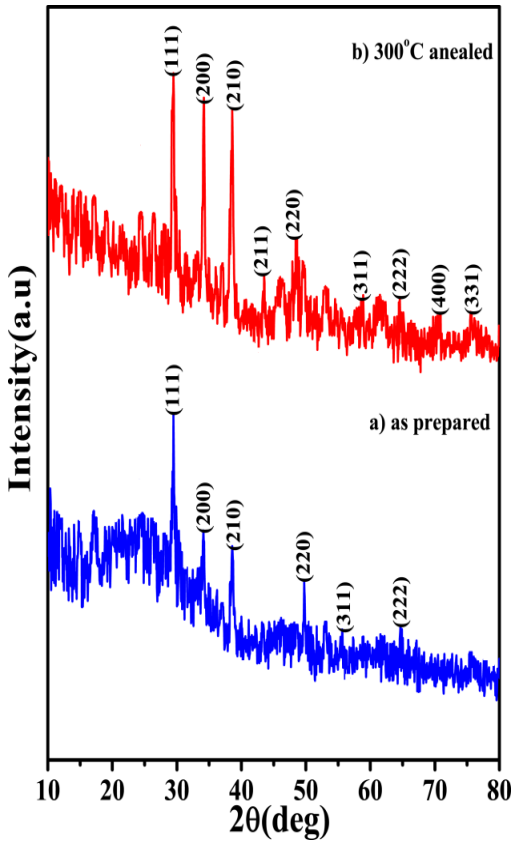

Fig 1. X-ray diffraction patterns of CdO biotemplates.

3.2 FTIR Spectral Analysis

The recorded FTIR absorbance spectra of as prepared and 300oC annealed CdO nanoparticle samples are shown in fig. 2(a, b) in the range 4000 cm-1 to 400 cm-1. Fig 2 (a) shows the presence of hydroxyl group absorbed at 3276 cm-1, 3353 cm-1, 3467 cm-1 and 3520 cm-1[31]. The sharp and broad peaks attributed at 1532 cm-1, 1589 cm-1 and 1637 cm-1 are due to the presence of C-O asymmetric vibrations. The C-O symmetric vibration mode appeared at 1222 cm-1 and 1402 cm-1[32]. The peaks observed around at 727cm-1, and 535 cm-1 confirm the Cd-OH Stretching and Cd-O Stretching[33, 34], respectively and shown in table 2. In fig 2(b) the presence of the Cd-O Stretching and Cd-OH Stretching are indicated by the absorption peaks at 439 cm-1[35], 510 cm-1 and 733 cm-1 for well evidence CdO. The peaks at 3276 cm-1 and 3353 cm-1 corresponding to hydroxyl functional group were removed by 300oC temperature treatment. The FTIR spectrum is good evidence for improved purity of CdO by annealing.

Table 1. The lattice spacing (d), full width at half maximum (FWHM), (hkl) planes, lattice constant and average particle size for CdO biotemplates.

As prepared						300° C annealed					
2θ	**d**	**FWHM**	**(hkl)**	**Lattice constant**	**Average Particle size**	**2θ**	**d**	**FWHM**	**(hkl)**	**Lattice constant**	**Average Particle size**
29.47	3.0309	0.2952	111	5.2496	23nm	29.36	3.0411	0.2952	111	5.2673	21nm
34.13	2.6268	0.3936	200	5.2536		34.18	2.6229	0.1968	200	5.2458	
38.60	2.3319	0.2952	210	5.2142		38.59	2.3328	0.3936	210	5.2162	
49.74	1.8329	0.2952	220	5.1842		42.44	2.0829	0.5904	211	5.1020	
56.40	1.7264	0.5904	311	5.7258		48.52	1.8763	0.2952	220	5.3069	
65.75	1.2530	0.5904	222	4.3405		56.01	1.7273	0.5904	311	5.7288	
-	-	-	-	-		64.42	1.5821	0.5904	222	5.4805	
-	-	-	-	-		70.20	1.4924	0.5904	400	5.9696	
-	-	-	-	-		75.83	1.2544	1.1808	331	5.4678	

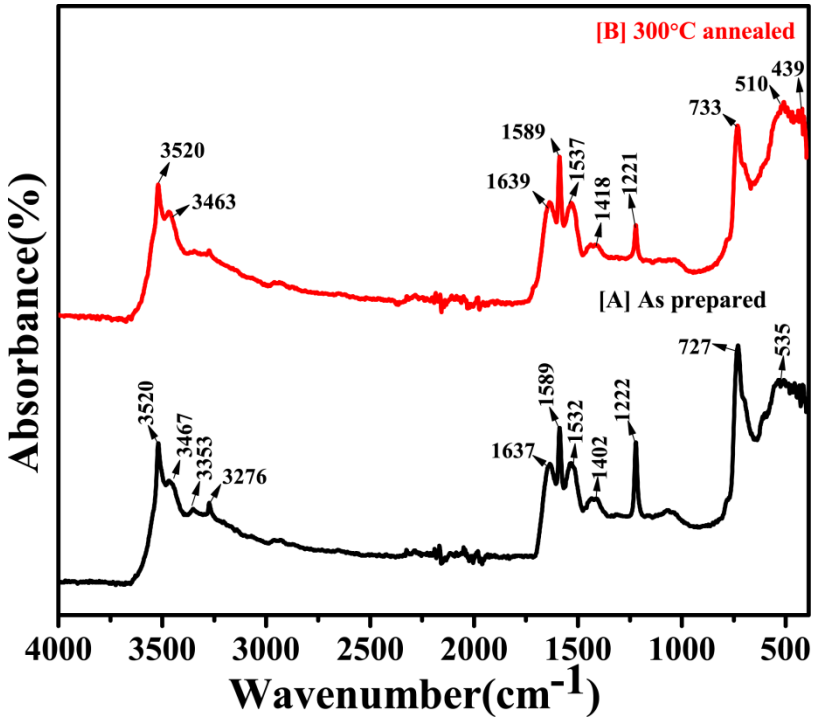

Fig 2. FT-IR spectrums of CdO biotemplates.

Table 2. FTIR assignments of CdO biotemplates.

Wavenumber(cm^{-1})		Peak assignments
A	**B**	
535	439 & 510	Cd-O Stretching
727	733	Cd-OH Stretching
1222 & 1402	1221 & 1418	C-O symmetric vibration
1532, 1589 & 1637	1537, 1589 & 1639	C-O asymmetric vibration
3276, 3353, 3467 & 3520	3463 & 3520	O-H Stretching

3.3 HRSEM Analysis

The surface morphology photos of the as prepared and 300ºC annealed CdO nanorods samples are shown in fig 3 and 4. SEM results show that the as prepared and 300ºC annealed CdO biotemplate have a crystalline nature with the formation of the CdO nanorods. Fig 3 shows the agglomerations of CdO have a large and rod shape regular crystals and fig 4 shows the annealed CdO has a closely packed and agglomerated rod shape regular crystals. The CdO nanorods crystalline sizes are in the range 15-30 nm as revealed by morphological analysis, which is found near to the calculated average particle size from XRD analysis. The obtained rod shape depends on the annealing process, which changes the agglomeration and particle size.

3.4 Transmission Electron Microscope Investigation

CdO nanorod morphology was investigated by TEM analysis. Fig 5 (a, b, and c) shows the morphology of as prepared CdO biotemplate (sample A). It is shown that the obtained CdO nanorods structure has a diameter of 10-100 nm and length of 500 nm with good crystalline nature. The 500 nm magnified image (fig 5c), revealed that the CdO nanorods were interconnected together and formed a good crystallinity. The insets of fig 5(a) and 5(c) show the evenly formed CdO nanorods at 200 nm magnification. The selected area diffraction pattern (inset fig 5b) indicates bright dots for a presence of the CdO biotemplate and it has a cubic phase structure. The distinct bright spots indicate a single crystalline nature of CdO biotemplate in accordance with the XRD results.

3.5 Energy Dispersive X-ray Spectroscopy (EDX) Analysis

Theenergy dispersive X-ray (EDX) spectrometer was used to investigate the elemental composition of the synthesized compound. Fig. 4 shows the recorded EDX spectra of as prepared CdO nanorods and 300oC annealed CdO nanorods. The recorded spectra confirmed the presence of Cd and O elements in the synthesized compound.
Fig.6a report the spectra of as prepared CdO which indicates a presence of Cd and O at a measured atomic percentage of elements 73.70% and 26.30% respectively. Fig. 6b shows the spectra of 300ºC annealed CdO with two peaks confirming the presence of Cd and O elements. The measured atomic percentages of these elements are75.86% and 24.14% respectively. From the EDX spectra shows while increasing the annealing process which places to reduce the oxygen in the synthesized compound.

3.6 UV-Visible-DRS Spectroscopy

The linear optical property of synthesized CdO biotemplate was studied by using UV-Visible- NIR spectrometer. The recorded UV-Vis-DRS spectra of as prepared and annealed CdO nanoparticles are shown in fig 7(a& b).The reflectance values were converted to absorbance by using the following Kubelka-Munk function

$$K = \frac{(1-\mathrm{R})^2}{2R} \qquad (2)$$

Where K is the reflectance transformed function according to Kubelka-Munk relation and R is the reflectance (%). The wavelength Vs (k*hυ)1/2 = f(h*υ) relationship spectra of as prepared and annealed CdO samples are shown in fig 8 (A&B). In the plot sample (a) has cutoff wave length 285 nm due to band gap energy 4.35 eV and sample (b) has cutoff wavelength 445 nm due to band gap energy 2.78 eV. This shows that increasing annealing temperature reduces the band gap energy of CdO biotemplate. It also shows decreases in the crystalline size due to a decrease of band gap energy.

3.7 Photoluminescence Studies

Room temperature Photoluminescence spectra of as prepared and 300ºC annealed CdO biotemplate were recorded on JY Fluorolog-FL3-11 spectrometer with Xenon lamp as a source. As shown in fig .9 (a-b). The excitation

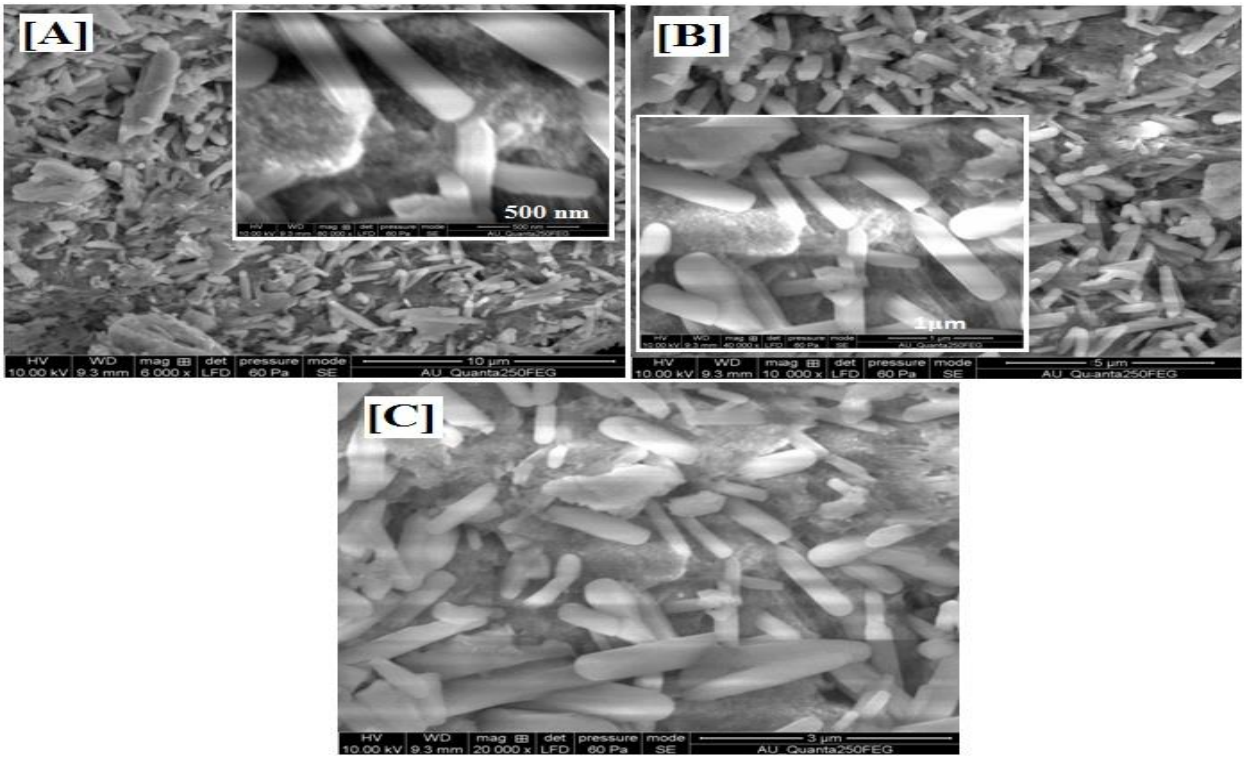

Fig 3. HRSEM images of as prepared CdO biotemplates.

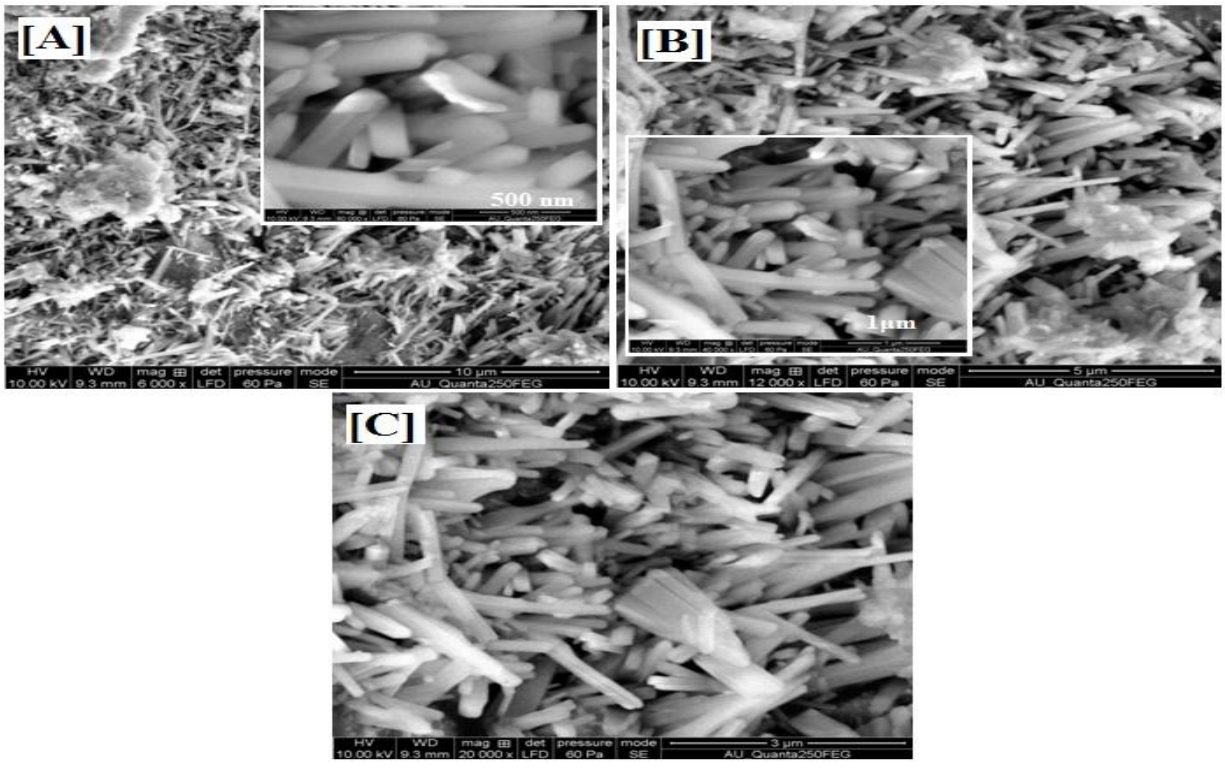

Fig 4. HRSEM images of 300ºC annealed CdO biotemplates.

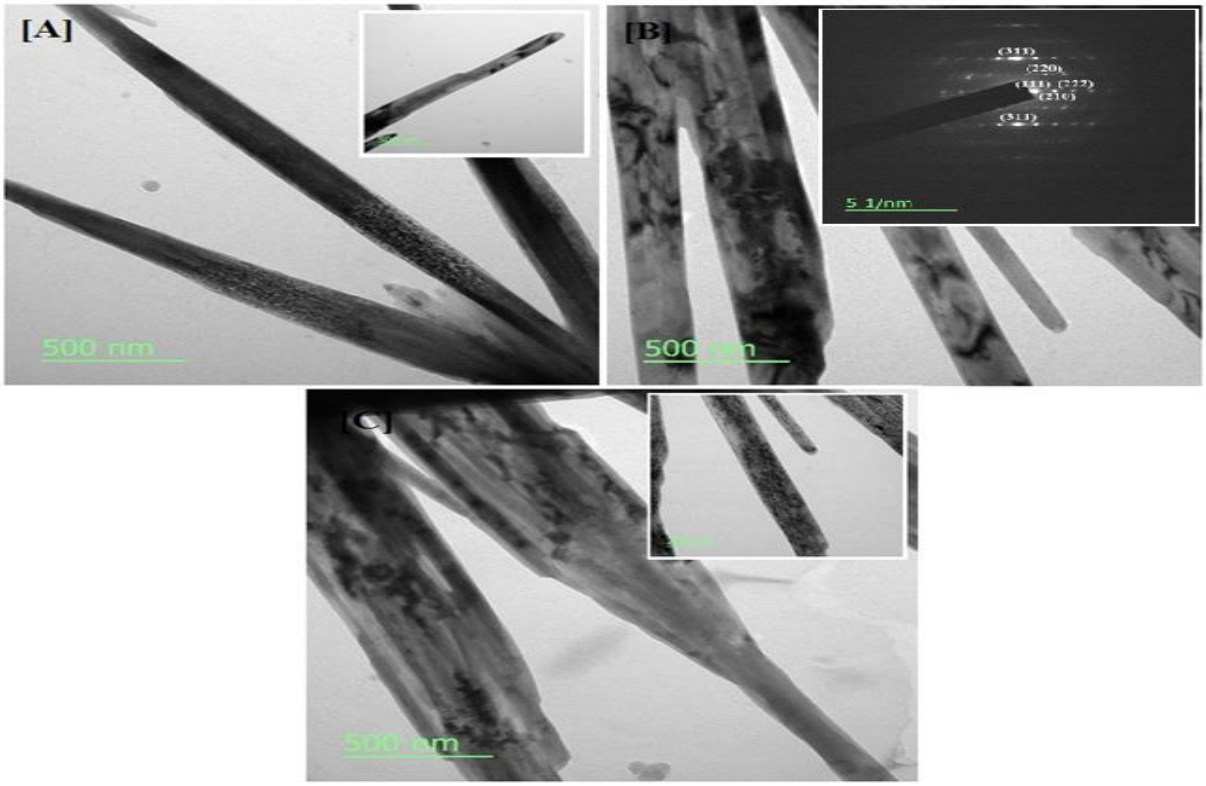

Fig 5. As prepared CdO biotemplate (sample A) TEM images (figure (A), (A) inset image, (B), (C), (C) inset image and figure B inset image is SAED pattern of CdO biotemplate.

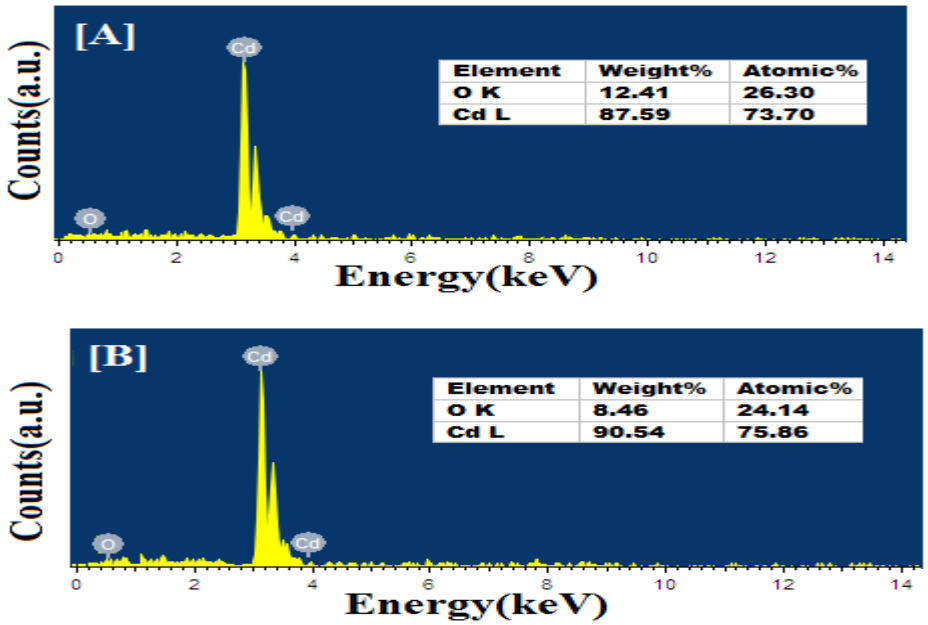

Fig 6. EDX spectra of (A) as prepared CdO nanorods and (B) 300°C annealed CdO nanorods.

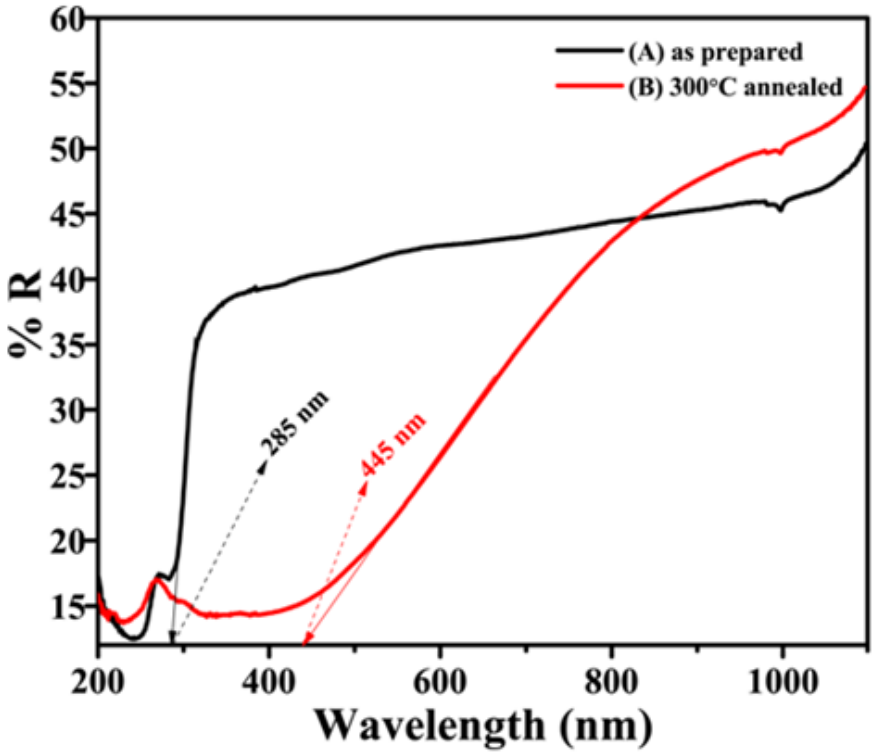

Fig 7. UV-DRS spectra of (A) as prepared CdO biotemplates and (B) 300°C annealed CdO biotemplates.

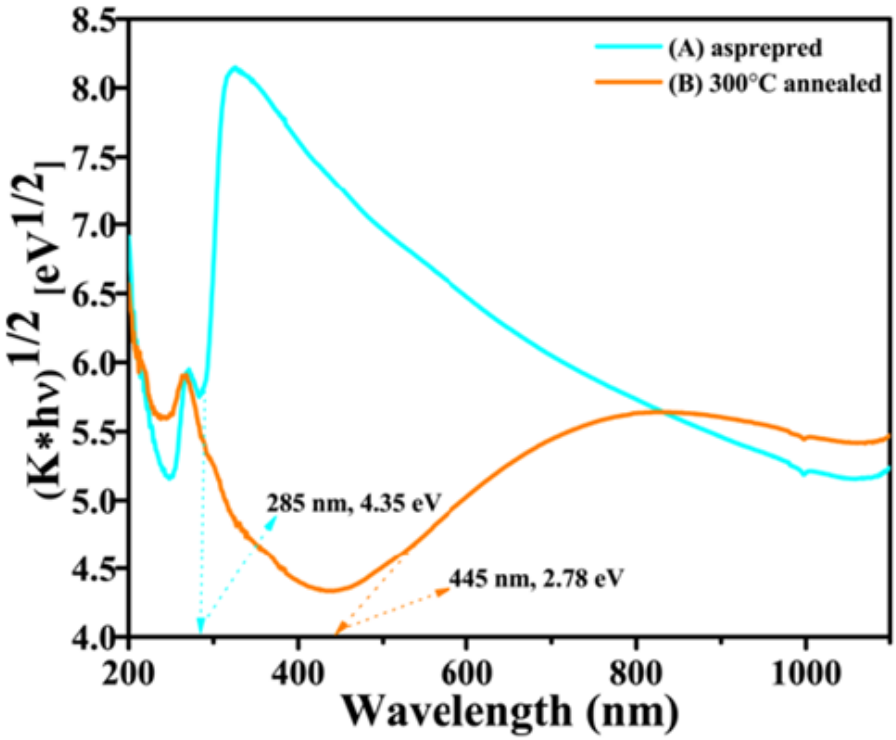

Fig 8. Wavelength (nm) Vs $(F(R)h\upsilon)^{1/2}$ spectrum of (A) as prepared CdO biotemplates and (B) 300°C annealed CdO biotemplates.

source wavelengths are in the range 15-30 nm 285nm for as prepared sample and 445nm for annealed sample. The excitation wavelength plays an important role in the electronic transition from highest occupied molecular orbital (HOMO) to the lowest unoccupied molecular orbital (LUMO) taking place for as prepared and annealed CdO biotemplate [36, 37]. Fig .9 (a) emission peak at 570nm (2.17eV) attribute for sharper green emission and Fig .9(b) emission peak observed at 529nm (2.34eV) for broad green emission [38]. Annealing process shifts the emission peak backward and increases the band gap. These results indicate that the synthesized CdO biotemplate can be used as suitable materials for LED applications.

3.8 Electrical Conductivity Measurements

The Keithley electrometer 6517B connected with a two probe setup was used to determine the electrical conductivity at different temperatures from 30-130°C (in order to deference 20°C). Figs 10. a& b illustrated the I-V characteristics of as prepared and annealed CdO biotemplates. In this spectra an indicated the current (I) value with increases temperatures at constant voltages (1-10 V). The electrical conductivity calculated by using the given equation (3) [38],

$$\sigma = \left(\frac{I}{V}\right) X \left(\frac{d}{A}\right) \qquad (3)$$

Where I is current, V is the applied voltage, d is the inter-probe distance and A is the cross sectional area of the pellet. Figs 11. a& b shows the temperature (°C) versus conductivity (S/cm). In this results reveals that conductivity an increases with annealed process at the range 5.50 x 10^{-9} to 1.04 10^{-8} and these results clearly revealed the semiconductors natures.

3.9 Anticancer Activity

3.9.1 In vitro Cytotoxicity Assay

The human cervical cancer cell line (HeLa) was obtained from National Centre for Cell Science (NCCS), Pune and grown in Eagles Minimum Essential Medium (EMEM) containing 10% fetal bovine serum (FBS). All cells were maintained at 37 ^{0}C, 5 % CO_2, 95 % air and 100 % relative humidity. Maintenance cultures were passaged weekly, and the culture medium was changed twice a week.

3.9.2 Cell Treatment procedure

The monolayer cells were detached with trypsin-ethylene diaminetetraacetic acid (EDTA) to make single cell suspensions and viable cells were counted by trypan blue exclusion assay using a hemocytometer. The cell suspension was diluted with medium containing 5 % FBS to give final density of 1x10^5 cells/ml. One hundred microlitres per well of cell suspension were seeded into 96-well plates at plating density of 10,000 cells/well and incubated to allow for cell attachment at 37 ^{0}C, 5 % CO_2, 95 % air and 100 % relative humidity. After 24h the cells were treated with serial concentrations (0.1-100 µM) of the test samples. They were initially dissolved in neat dimethylsulfoxide (DMSO) and diluted to twice the desired final maximum test concentration with serum free medium. Additional four, serial dilutions were made to provide a total of five sample concentrations. Aliquots of 100 µL of these different sample dilutions were added to the appropriate wells already containing 100 µL of medium, resulted the required final sample concentrations. Following drug addiction the plates were incubated for an additional 48h at 37 ^{0}C, 5 % CO_2, 95 % air and 100 % relative humidity. The medium containing without samples were served as control and triplicate was maintained for all concentrations.

3.9.3 MTT Assay

3-[4,5-dimethylthiazol-2-yl]2,5-diphenyltetrazolium bromide (MTT) is a yellow water soluble tetrazolium salt. A mitochondrial enzyme in living cells, succinate-dehydrogenase, cleaves the tetrazolium ring, converting the MTT to an insoluble purple formazan. Therefore,the amount of formazan produced is directly proportional to the number of viable cells. After 48h of incubation, 15 µL of MTT (5 mg/ml) in phosphate buffered saline (PBS) was added to each well and incubated at 37 ^{0}C for 4h. The medium with MTT was then flicked off and the formed formazan crystals were solubilized in 100 µL of DMSO and then measured the absorbance at 570 nm using micro plate reader. The % cell inhibition was determined using the following formula.

% Cell Inhibition = 100- Abs (sample)/Abs (control) x100

Nonlinear regression graph was plotted between % Cell inhibition and Log concentration (Fig.12) and IC50 was determined using Graph Pad Prism software [39, 40].

The cytotoxicity of newly synthesized compounds against human cervical cancer cell line (HeLa) was evaluated by means of MTT assay method. This method measures mitochondrial dehydrogenase activity as an indication of cell viability (corresponding to the reductive activity) and is proportional to the production of purple formazan, which is measured spectrophotometrically [41]. The results are analyzed by means of cell viability curves and expressed with IC_{50} (the concentration that cause a 50 % reduction of the cell growth) values whose concentration ranges from 0.1-100 µM. The growth inhibition (%) obtained with continuous exposure for 48h. The cytotoxicity of compounds was found to be concentration dependent. The growth inhibition increased with increasing the concentration of CdO biotemplate. In the present study, the antitumor effects of the CdO biotemplate against human cervical cancer cell line (HeLa). In this study, we

investigate the effect of CdO biotemplate on cytotoxicity effect as shown in Fig. 13. CdO NPs exerted significant cytotoxicity effect on cancer cells in dose dependent manner. The IC50 value of CdO biotemplate on HeLa cancer cell line was 38.76 µM. From this results suggested that the CdO biotemplate possessed potent cytotoxicity against HeLa cancer cell line.

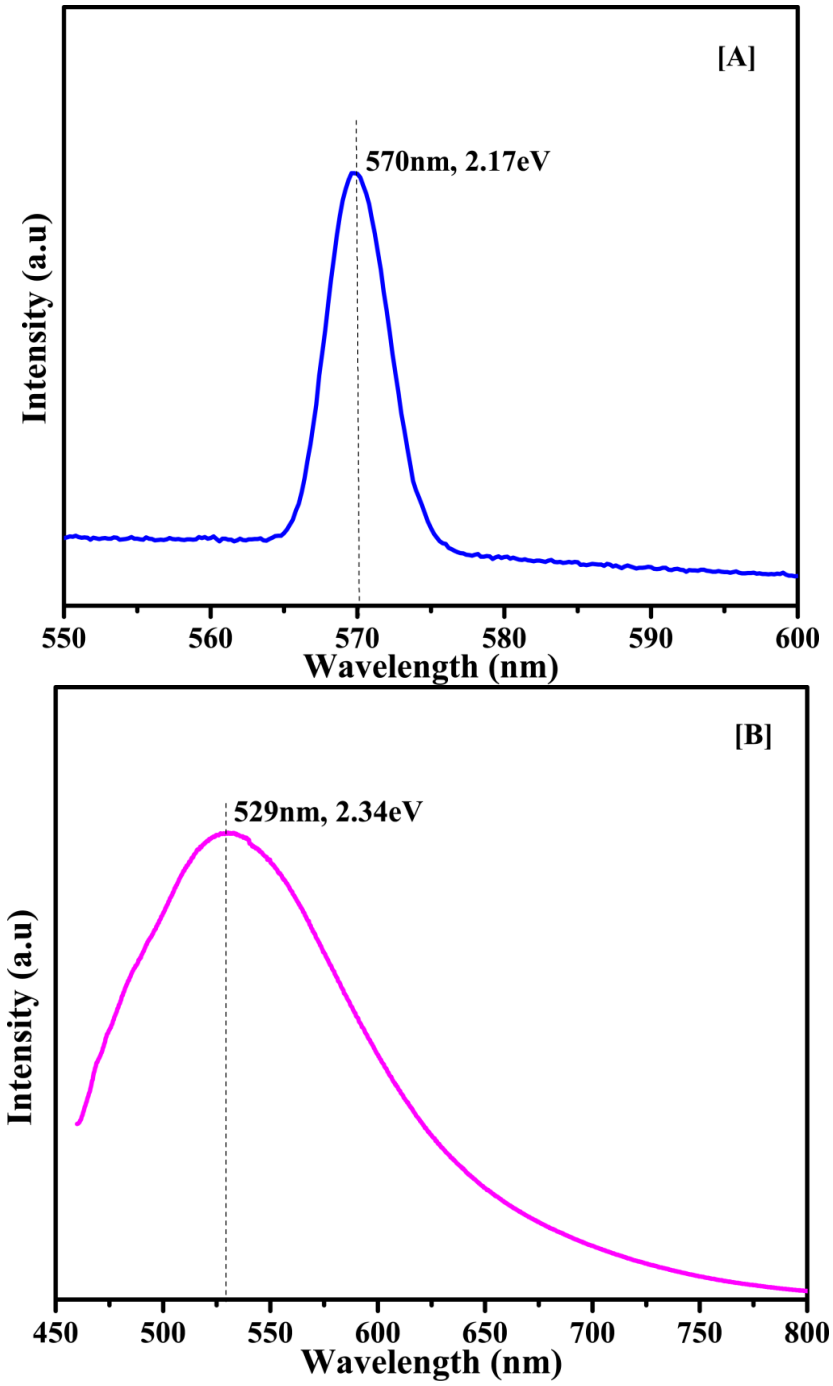

Fig 9. PL spectra of (A) as prepared CdO biotemplates and (B) 300°C annealed CdO biotemplates.

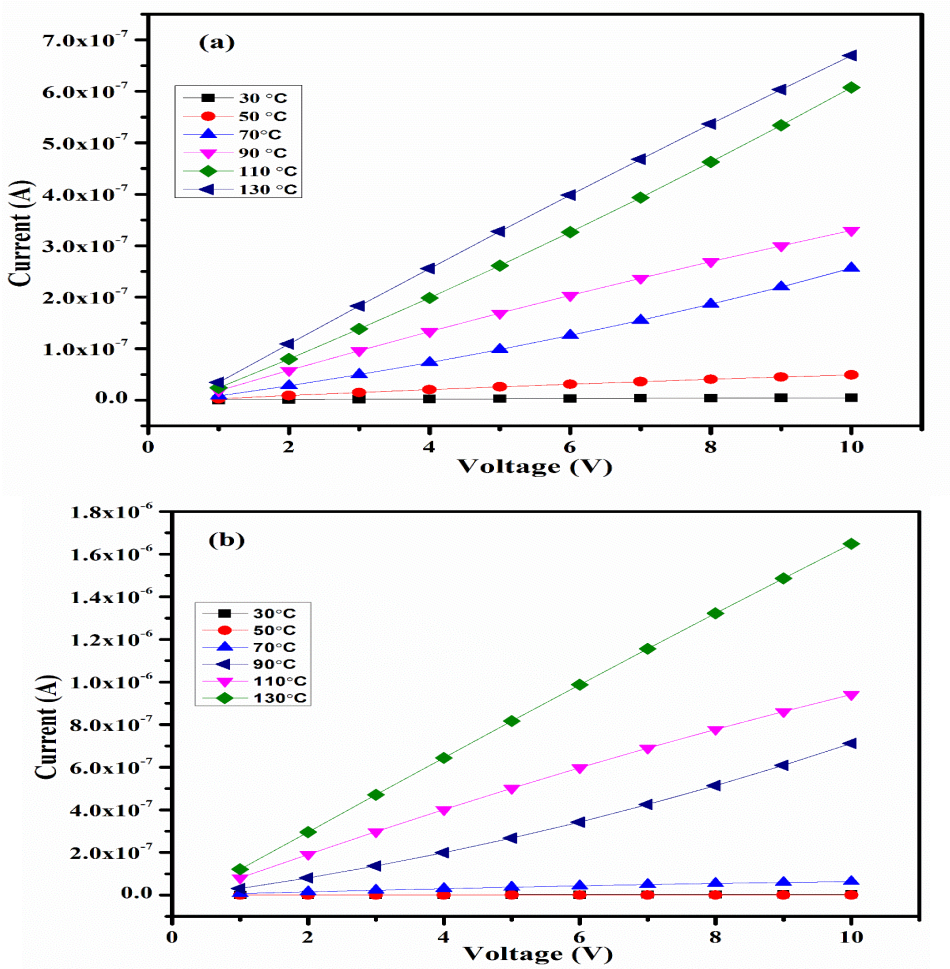

Fig 10. I-V spectra of (A) as prepared CdO biotemplates and (B) 300ºC annealed CdO biotemplates.

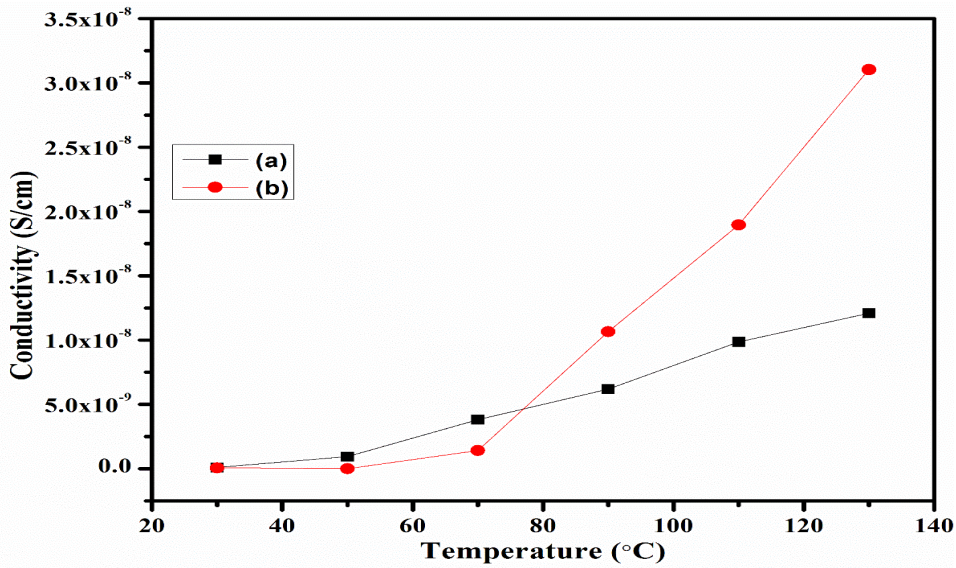

Fig 11. Temperature (°C) versus Conductivity (S/cm) spectra of (A) as prepared CdO biotemplates and (B) 300ºC annealed CdO biotemplates.

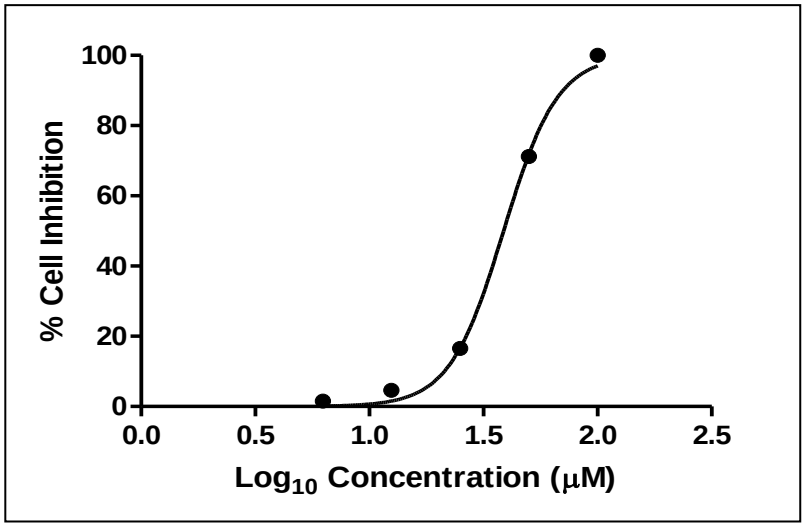

Fig 12. Plot of the % growth cell inhibition at various concentrations.

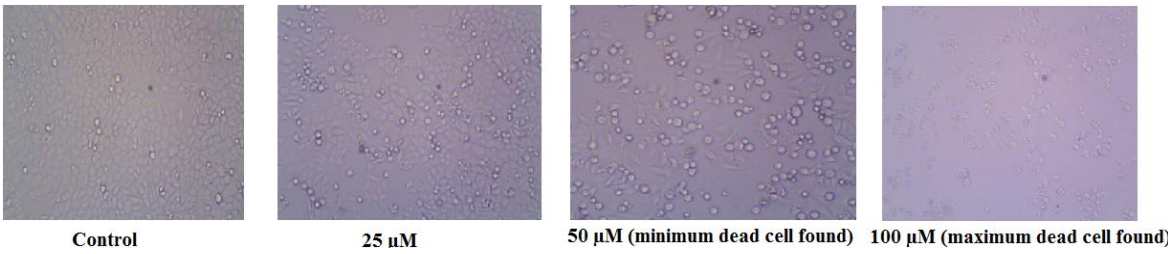

Fig13. Morphological changes of cancer cells (human cervical cancer, HeLa) induced by CdO nanoparticals**.**

4 Conclusions

The rod shaped CdO biotemplate was successfully synthesized by chemical rout assisted microwave irradiation method via Hen egg albumen extract. An annealing at 300 ^{o}C for 2h under the muffle furnace produces CdO with high crystallite cubic phase. The XRD analysis confirmed the cubic phase and high crystallite property. The FTIR and EDX measurements data are good evidence for CdO and albumen precipitates. The rod shape morphology observed from HRSEM and TEM report and high crystallite property also conformed from annealed CdO biotemplate by HRSEM image. The annealing process reduced the band gap from 4.35eV to 2.78eV which is confirmed by UV-Vis DRS analysis. The strong green emission peaks at 570nm and 529nm are got in room temperature PL analysis. The conductivity increases with annealed process at the range 5.50 x 10^{-9} to 1.04 10^{-8} and these results clearly revealed the semiconductors natures. These studies indicate that the rod shaped CdO biotemplate is potentially useful for optoelectronic and biological applications.

Acknowledgment

We acknowledge Dr. N. Athirajan, Assistant Professor, Cell Culture Laboratory, KMCH College of Pharmacy, Coimbatore for evaluating cytotoxicity.

References

[1] Zai-Xing Yang, Wei Zhong, Yan-Xue Yin, Du Xin, Yu Deng, Chaktong Au, You- Wei Du, Controllable Synthesis of Single-Crystalline CdO and Cd(OH)2Nanowires by a Simple Hydrothermal Approach, Nanoscale Res. Lett. **5** (2010) 961–965.

[2] F. Saito, Q. Zhang, J. Kano,Mechanochemical approach for preparing nanostructural materials, J. Mater. Sci. **39** (2004) 5051–5055.

[3] F. Yakuphanoglu, Nanocluster n-CdO thin film by sol–gel for solar cell applications, Appl. Surf. Sci. **257** (2010) 1413–1419.

[4] R. S. Mane, H. M. Pathan, C. D. Lokhande, S.H. Han, An effective use of nanocrystalline CdO thin films in dye-sensitized solar cells, Sol. Energy **80** (2006) 185–190.

[5] T. V. S. Sarma, S. Tao, An active core fiber optic sensor for

detecting trace H2S at high temperature using a cadmium oxide doped porous silica optical fiber as a transducer, Sens. Actuat. B: Chem. **127** (2007) 471–479.

[6] R. R. Salunkhe, C. D. Lokhande, Effect of film thickness on liquefied petroleum gas (LPG) sensing properties of SILAR deposited CdO thin films, Sens Actuat B: Chem. **129** (2008) 345–351.

[7] M. H. Kim, Y.U. Kwon, Semiconductor CdO as a Blocking Layer Material on DSSC Electrode: Mechanism and Application, J. Phys. Chem. C **113** (2009) 17176–17182.

[8] F. Yakuphanoglu, M. Caglar, Y. Caglar, S. Ilican, Electrical characterization of nanocluster n-CdO/p-Si heterojunction diode, J. Alloys Compd. **506** (2010) 188–193.

[9] X. Liu, C. Li, S. Han, J. Han, C. Zhou, Synthesis and electronic transport studies of CdO nanoneedles, Appl. Phys. Lett. **82** (2003) 1950–1952.

[10] S. M. Pawar, B. S. Pawar, J. H. Kim, O. S. Joo, C. D. Lokhande, Recent status of chemical bath deposited metal chalcogenide and metal oxide thin films, Current Appl. Phys**11** (2011) 117–161.

[11] J. Li, Y. Ni, J. Liu, J. Hong, Preparation, conversion, and comparison of the photocatalytic property of Cd (OH) 2, CdO, CdS and CdSe, J PhysChem Solid **70** (2009) 1285–1289.

[12] W. Dong, C. Zhu, Optical properties of surface-modified CdO nanoparticles, Opt. Mater. **22** (2003) 227–233.

[13] K. Manickathai, S. K. Viswanathan, M. Alagar, Optical properties of surface-modified CdO nanoparticles, Indian J. Pure Appl. Phys. **46** (2008) 561–564.

[14] A. Askarinejad, A. Morsali, Synthesis of cadmium (II) hydroxide, cadmium (II) carbonate and cadmium (II) oxide nanoparticles; investigation of intermediate products, Chem. Eng. J. **150** (2009) 569–571.

[15] M. Ghosh, C. N. R. Rao, Solvothermal synthesis of CdO and CuO nanocrystals, Chem. Phys. Lett. **393** (2004) 493–497.

[16] H. Yang, G. Qiu, X. Zhang, A.Tang, W.Yang, Preparation of CdO nanoparticles by mechanochemical reaction, J. Nanopart. Res. **6** (2004) 539–542.

[17] A. Tadjarodi, M. Imani, Synthesis and characterization of CdO nanocrystalline structure by mechanochemical method, Mater. Lett. **65** (2011) 1025–1027.

[18] A. Tadjarodi, M. Imani, A novel nanostructure of cadmium oxide synthesized by mechanochemical method, Mater. Res. Bull. **46** (2011) 1949–1954.

[19] M. B. Dickerson, K. H. Sandhage, R. R. Naik, Protein-and peptide-directed syntheses of inorganic materials, Chem. Rev. **108** (2008) 4935–4978.

[20] T. Prakash, R. Jayaprakash, D. Sathya Raj, Sanjai Kumar, N. Donato, D. Spadaro, G. Neri, Sensing properties of ZnO nanoparticles synthesized by using albumen as a biotemplate for acetic acid monitoring in aqueous mixture, Sens. Actuators, B **176** (2013) 560–568.

[21] T. Prakash, R. Jayaprakash, G. Neri, Sanjai Kumar, A comparative study of the synthesis of CdO nanoplatelets by an albumen-assisted isothermal evaporation method, J. Nanopart. **8** (2013) (Article ID 274894).

[22] Peng Huang, Le Bao, Dapeng Yang, Guo Gao, Jing Lin, Zhiming Li, Chunlei Zhang, Daxiang Cui, Protein‐Directed Solution‐Phase Green Synthesis of BSA‐Conjugated MxSey (M= Ag, Cd, Pb, Cu) Nanomaterials, Chem. Asian J. **6** (2011) 1156–1162.

[23] S. Somiya, K. Hishinuma, T. Akiba, A new materials processing—hydrothermal processing, Bull. Mater. Sci. **6** (1995) 811–818.

[24] M. M. Lencka, R. E. Riman, Thermodynamic modeling of hydrothermal synthesis of ceramic powders, Chem. Mater. **5** (1993) 61–70.

[25] M. A. Gabal, Structural and magnetic properties of nano-sized Cu–Cr ferrites prepared through a simple method using egg white, Mater. Lett. **64** (2010) 1887–1890.

[26] S. M. Senthil, R. Jayaprakash, V. N. Singh, B. R. Mehta, G. Govindaraj, Synthesis and magnetic properties of nanosized cobalt substituted nickel ferrites (Ni1-xCoxFe2O4) using egg white (ovalbumin) by thermal evaporation, Nano Res. **4** (2008) 107–116.

[27] S. M. Senthil, R. Jayaprakash, S. R. Murthy, A. R. Phani, V. N. Singh, G. Govindaraj, Effect of Annealing on Dielectric Property in Ni1-xCoxFe2O4 Nanoparticles Synthesized using Albumen (egg white), Nano Res. **6** (2009) 205–213.

[28] Z. Durmus, A. Baykal, H. Kavas, M. Direkçi, M.S. Toprak, Ovalbumin mediated synthesis of Mn3O4, Polyhedron **28** (2009) 2119–2122.

[29] FatemehNouroozi, FaezehFarzaneh, Synthesis and characterization of brush-like ZnO nanorods using albumen as biotemplate, J. Braz. Chem. Soc. **22** (2011) 484–488.

[30] Santi Maensiri, ChivalratMasingboon, PaveenaLaokul, WiratJareonboon, VinichPromarak, Philip L. Anderson, SupapanSeraphin, Egg white synthesis and photoluminescence of platelike clusters of CeO2 nanoparticles, Cryst. Growth Des. **7** (2007) 950–955.

[31] S. Gandhi, R. H. H. Subramani, T. Ramankrishnan, A. Sivabalan, V. Dhanalakshmi, M.R.G. Gopinath Nair, R. Anbarasan, Ultrasound assisted one pot synthesis of nano-sized CuO and its nanocomposite with poly (vinyl alcohol), J. Mater. Sci. **45** (2010) 1688–1694.

[32] K. Mohanraj, D. Balasubramanian, J. Chandrasekaran, B. Babu, Structural, morphological, optical and electrical properties of nail-shaped CdO nanoparticles synthesized by chemical route assisted microwave irradiation method for P–N junction diode application, J Mater Sci: Mater Electron (2017) **28**:7749–7759.

[33] B. Malecka, A. Lacz, Thermal decomposition of cadmium formate in inert and oxidative atmosphere, ThermochimicaActa **479** (2008) 12-16.

[34] R. K. Swarnkar, S. C. Singh, R. Gopal, Synthesis of Copper/Copper‐Oxide Nanoparticles: Optical and Structural Characterizations, AIP Conf. Proc. **1147** (2009)205–210.

[35] Y. Lei, L.D. Zhang, G.W. Meng, G. H. Li, X. Y. Zhang, C.

H. Liang, W. Cheng, S.X. Wang, Preparation and photoluminescence of highly ordered TiO2 nanowire arrays, Appl.Phys.Lett. **78** (2001) 1125.

[36] B. L. Tian, X.T. Zhang, S. X. Dai, K. Cheng, Z. S. Jin, Y. B. Huang, Z. L. Du, G.T. Zou, B. S. Zou, Strong visible absorption and photoluminescence of titanic acid nanotubes by hydrothermal method, J. Phys. Chem. C**112** (2008) 5361.

[37] I. R. Chavez Urbiola, R. Ramirez Bon, Y.V. Vorobiev, The transformation to cadmium oxide through annealing of cadmium oxide hydroxide deposited by ammonia-free SILAR method and the photocatalytic properties, Thin Solid Films **592** (2015) 110-117.

[38] M. Balaji, J. Chandrasekaran, M. Raja, Role of substrate temperature on MoO 3 thin films by the JNS pyrolysis technique for P–N junction diode application, Mater. Sci. Semicond. Process. **43** (2016) 104–113.

[39] T. Mossman,Rapid colorimetric assay for cellular growth and survival: application to proliferation and cytotoxicity assays, J Immunol Methods **65** (1983) 55-63.

[40] A. Monks, D. Scudiero, P. Skehan, R. Shoemaker, K. Paull, D. Vistica, C. Hose, J. Langley, P. Cronise, A. Vaigro-Wolff, M. Gray-Goodrich, H. Campbell, J. Mayo,Michael Boyd,Feasibility of a High-Flux Anticancer Drug Screen Using a Diverse Panel of Cultured Human Tumor Cell Lines, JNCI **83** (1991) 757-766.

[41] V. Moreno, M. F. Bardia, T. Calvet, J. Lorenzo, F. X. Aviles, M. H. Garcia, T. S. Morais, A. Valente, M. P. Robalo, DNA interaction and cytotoxicity studies of new ruthenium (II) cyclopentadienyl derivative complexes containing heteroaromatic ligands, J InorgBiochem**105** (2011) 241 - 249.